Kinematic Calibration of Linear-Actuated Parallel Mechanisms from Leg Observation

Pierre Renaud, Nicolas Andreff, Sébastien Krut, Grigoré Gogu

Kinematic calibration of linear-actuated parallel mechanisms from leg observation

Pierre Renaud[1], Nicolas Andreff[1,2], Sébastien Krut[3], Grigore Gogu[1]

[1]*LaRAMA, Université Blaise Pascal/IFMA, Clermont-Ferrand, France, renaud/andreff@ifma.fr*
[2]*LASMEA, Université Blaise Pascal/CNRS, Clermont-Ferrand, France*
[3]*LIRMM, Université Montpellier II / CNRS, Montpellier, France, krut@lirmm.fr*

Abstract

In this article, an original algorithm is proposed to achieve the kinematic calibration of parallel mechanisms with linear actuators on the base, using vision as an exteroceptive sensor to perform measurements on the legs of the mechanism. The calibration can be performed without adding proprioceptive sensors or restricting the mechanism's workspace during the calibration process. The algorithm is implemented for the calibration of the I4 parallel mechanism with experimental results.

1 Introduction

Among the proposed architectures for parallel mechanisms, structures with linear actuators on the base are of great interest: inertial effects are lowered, and the use of modern linear actuators allows us to build mechanisms with high dynamics. Consequently, many recently developed structures belong to this class of mechanisms such as Hexaglide [1], I4 [2], Orthoglide [3]. Their use is highly dependent on their accuracy. Compared to serial mechanisms, they may exhibit a much better repeatability [4], but not necessarily a better accuracy, because of their large number of links and passive joints [5]. A kinematic calibration is thus needed for these structures.

The various approaches proposed to perform the kinematic calibration of parallel mechanisms are based on the minimization of an error function which depends on a geometrical parameter vector defining the mechanism. With error functions expressed using the direct kinematic model, numerical models have generally to be used, leading to stability and convergence problems in the identification process [6]. With methods based on the inverse kinematic model, the full pose of the end-effector has to be measured, which is often complex and tedious to achieve accurately. Vision can be an adequate sensor [7]. The calibration efficiency is however limited for a large mechanism workspace, as the measurement accuracy lowers, and the calibration procedure seems rather difficult to achieve online: the end-effector is generally inaccessible or its observation impossible because of the environment, with for instance lubricant projections in a machine-tool. Alternative methods are based on additional measurements on the passive links [8, 9, 6, 10, 11], or mechanical constraints on some elements of the mechanism [11, 12, 13]. However the former method is not always economically and technologically achievable and the involvement of mechanical constraints implies a significant reduction of the workspace during the calibration, which lowers the quality of the identification.

We recently proposed [14] to get information redundancy by observing with a camera the legs that connect the actuators to the end-effector. No mechanical modification or workspace limitation is then needed, and calibration can be performed online since the end-effector observability is not needed. The kinematics of parallel mechanisms are furthermore intrinsically linked to the kinematics of their legs. In this article, we introduce a calibration method based on the leg observation for mechanisms with linear actuators on the base. For sake of clarity, the algorithm is presented in the context of the I4 parallel mechanism. A more general algorithm may be found in [15].

In the second part, the I4 parallel mechanism is presented with its modeling. In the third part the calibration algorithm is then detailed. Experimental results are given in the fourth part, before concluding on the performance and further developments of the identification method.

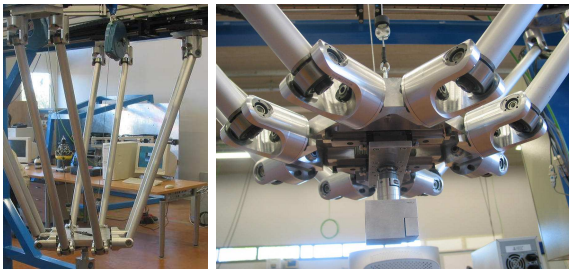

(a) General view (b) Traveling plate view

Figure 1: *The I4 mechanism - General view and traveling plate.*

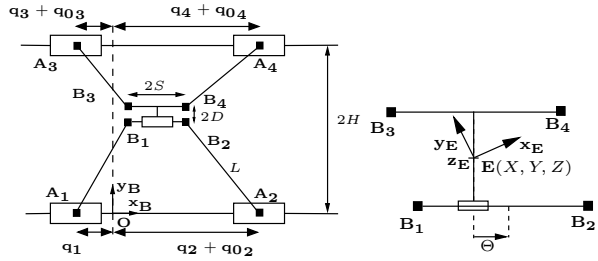

(a) Mechanism (b) Traveling plate

Figure 2: *I4 mechanism geometry.*

2 Mechanism Modeling

2.1 Mechanism structure

The I4 mechanism [2] is a four degree-of-freedom mechanism actuated by four linear actuators fixed on the base (figure 1(a)). Four legs, made with articulated parallelograms, link the actuators to a traveling plate which supports the end-effector. The end-effector can be translated in three directions, and rotated by the relative displacement of the two plate parts (figure 1(b)), using two rack-and-pinion systems. The workspace volume is approximately equal to $500 \times 400 \times 400\ mm^3$ with a 360° end-effector rotation.

2.2 Modeling assumptions

Wang and Masory [5] have shown that the influence of the joint defects on the mechanism accuracy is negligible compared to the influence of the joint positioning errors for a Stewart-Gough platform. This result is considered valid in our context, so that the mechanism geometry is defined by the relative positions of the joint characteristic elements. For the prismatic joints, these characteristic elements are the unit vectors of their axis and the position of a point on the joint axis. The spherical joints are defined by their centers.

The articulated parallelograms are considered perfect, which means that their sides stay parallel by pairs. They can then be defined for the calibration by kinematically equivalent single rods of same length linked in $\mathbf{A_j},\ \mathbf{j} \in [1,4]$ and $\mathbf{B_j},\ \mathbf{j} \in [1,4]$ (figure 2(a)).

Because of the manufacturing tolerances, some assumptions achieved during the design of the mechanism are considered valid for the calibration. The actuator axes are considered parallel and coplanar, as well as the point $\mathbf{A_j},\ \mathbf{j} \in [1,4]$, and located on two lines (figure 2(a)). The four kinematically equivalent single rods are considered identical with a length L.

The elements observed with the camera are those connected to the traveling plate. The axes of these cylindrical elements and the lines joining the points $\mathbf{A_j}$ and $\mathbf{B_j},\ \mathbf{j} \in [1,4]$ are considered parallel.

2.3 Parameterization

The base frame $R_B(\mathbf{O}, \mathbf{x_B}, \mathbf{y_B}, \mathbf{z_B})$ is defined using as frame origin the joint center $\mathbf{A_1}$ position when the encoder value of the corresponding actuator is equal to zero (*i.e.* $\mathbf{O} = \mathbf{A_1}|_{\mathbf{q_1}=\mathbf{0}}$). The four points $\mathbf{A_j},\ \mathbf{j} \in [1,4]$ are located in the $(\mathbf{x_B}, \mathbf{y_B})$ plane and line $\mathbf{A_1A_2}$ is parallel to the $\mathbf{x_B}$ axis.

The end-effector frame $R_E(\mathbf{E}, \mathbf{x_E}, \mathbf{y_E}, \mathbf{z_E})$ is defined with its origin located at the intersection between the revolute joint axis and the plane containing the points $\mathbf{B_j},\ \mathbf{j} \in [1,4]$ (figure 2(b)). The orientation of the vectors $\mathbf{x_E}$ and $\mathbf{y_E}$ is selected to be the same as $\mathbf{x_B}$ and $\mathbf{y_B}$ when the lines $\mathbf{B_1B_3}$ and $\mathbf{B_2B_4}$ are parallel to $\mathbf{y_B}$. The end-effector pose is defined by the position (X, Y, Z) of the end-effector frame origin and its orientation Θ with respect to the base frame.

Finally, four parameters are needed to define the joints on the base: the distance $2H$ between the two actuator axes and three encoder offsets $\mathbf{q_{0j}}, \mathbf{j} \in [2,4]$ so that:

$$(\mathbf{OA_j}) \,.\mathbf{x_B} = \mathbf{q_j} + \mathbf{q_{0j}} \tag{1}$$

The relative position of the joint centers $\mathbf{B_j},\ \mathbf{j} \in [1,4]$ is defined by the dimensions S and D. Seven parameters finally define the mechanism geometry: $(H, \mathbf{q_{02}}, \mathbf{q_{03}}, \mathbf{q_{04}}, S, D, L)$.

Step 1	Base parameter estimation in the camera frame $\rightarrow (\mathbf{A_j^0})_{R_C}$
Step 2	Parameter estimation in the base frame $\rightarrow (\mathbf{q_{02}}, \mathbf{q_{03}}, \mathbf{q_{04}}, H)$
Step 3	Estimation of the length of the kinematically equivalent single rods connected to the traveling plate $\rightarrow L$
Step 4	Estimation of the parameters of the traveling plate $\rightarrow (S, D)$

Table 1: *The calibration method structure*

3 Calibration method

To identify the mechanism kinematic parameters described in the former section, we propose a calibration method using a camera to observe the cylindrical elements constituting the articulated parallelograms connected to the traveling plate. One can demonstrate that the observation of a cylindrical element enables us to determine its pose with respect to the camera frame [14], *i.e.* the position and the orientation of the axis of the element. It must be outlined that the camera location is not considered to be known accurately, which enables a simple experimental procedure.

The method is composed of four steps (table 1). The first one is performed to get information in the camera frame and the kinematic parameters are determined in the three following steps. Steps 2 and 3 are actually independent, which tends to minimize the error propagation in the calibration process.

3.1 Step 1 - Base parameter estimation in the camera frame

In the first step, the locations of the points $\mathbf{A_j},\ \mathbf{j} \in [1,4]$ are identified in the camera frame. Due to modeling assumptions, this also implies the identification of the actuator axes.

The end-effector is moved to modify the orientation of the legs, while locking an actuator j in a position m (figure 3). The observation of the two corresponding cylindrical elements in N_I different orientations enables one to measure their axes $\underline{\mathbf{u}}_{\mathbf{j,k}}$ and $\underline{\mathbf{u}'}_{\mathbf{j,k}}$, $\mathbf{k} \in [1, N_I]$ and the position of points $\mathbf{M_{j,k}}$ and $\mathbf{M'_{j,k}}$ on their axes. The position of the spherical joint centers $\mathbf{P_{j,m}}$ and $\mathbf{P'_{j,m}}$ can hence be computed in the camera frame by expressing their belonging to the axes:

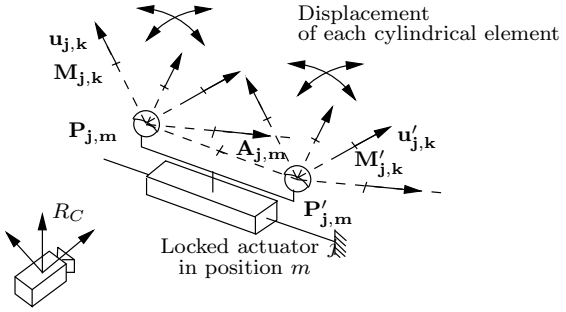

Figure 3: *Identification of the joint centers in the camera frame.*

$$\left.\begin{array}{r} \mathbf{P_{j,m}M_{j,k}} \times \underline{\mathbf{u}}_{\mathbf{j,k}} = \mathbf{0} \\ \mathbf{P'_{j,m}M'_{j,k}} \times \underline{\mathbf{u}'}_{\mathbf{j,k}} = \mathbf{0} \end{array}\right\} \ \mathbf{k} \in [1, N_I] \qquad (2)$$

The position of the joint center $\mathbf{A_{j,m}}$ is then easily determined:

$$\mathbf{A_{j,m}} = \frac{\mathbf{P_{j,m}} + \mathbf{P'_{j,m}}}{2} \qquad (3)$$

The coordinates of $\mathbf{A_{j,m}}$ in the camera frame can therefore be computed after solving the overdetermined linear system obtained by concatenation of the $6N_I$ vector equations (2). As the equations provided by the cross product for each pose are not independent, the solution is obtained by a singular value decomposition. It can be easily proved that two leg orientations are at least necessary to estimate the joint center position: $N_I \geq 2$

Locking sequentially the four actuators, the position of the points $\mathbf{A_j}, \mathbf{j} \in [1,4]$ can be determined for the known position of the associated actuator.

Since the points $\mathbf{A_1}$ and $\mathbf{A_2}$ are aligned with the actuator axes, as well as $\mathbf{A_3}$ and $\mathbf{A_4}$, the actuator axis $\mathbf{x_B}$ is determined in the camera frame from the knowledge of the location of the points $\mathbf{A_j},\ \mathbf{j} \in [1,4]$. The position of the points $\mathbf{A_j},\ \mathbf{j} \in [1,4]$ can hence be determined for any position of the actuator, and in particular when the encoder value is equal to zero. The unit vector $\mathbf{z_B}$ perpendicular to the plane containing the joint centers can be computed at the same time, and consequently the unit vector $\mathbf{y_B}$ too.

3.2 Step 2 - Parameter estimation in the base frame

At the end of the first step, the position of the points $\mathbf{A_j},\ \mathbf{j} \in [1,4]$ and the actuator axes are determined in the camera frame. Expressing these elements in the base frame requires the knowledge of the camera pose

with respect to the base. Designing a system to impose accurately the camera location would be expensive and its use restricting, so that this location is computed. This computation can be achieved explicitly, introducing the corresponding unknowns, or implicitly by directly searching the kinematic parameters in the base frame. The latter solution is selected since it enables one to suppress the need of *a priori* knowledge of the transformation ${}^{B}T_{C}$, which is of great interest as the camera frame is not physically measurable.

To determine the kinematic parameters in the base frame, an error function is expressed using the invariance of the scalar product with Euclidian transformation. Scalar products are expressed both in the base frame and in the successive camera frames.

The position of the joint centers $\mathbf{A_j},\ \mathbf{j} \in [1,4]$ when the actuator encoder values are equal to zero are estimated in the previous step in the camera frame. From these four positions $\mathbf{A_j^0},\ \mathbf{j} \in [1,4]$, three independent vectors $\mathbf{A_j^0 A_g^0},\ (\mathbf{j},\mathbf{g}) \in [1,4]$ can be computed. One can then constitute a vector set $\mathbf{V}$ of independent vectors:

$$\mathbf{V} = \left(\mathbf{A_1^0 A_2^0}, \mathbf{A_1^0 A_3^0}, \mathbf{A_1^0 A_4^0}\right) \tag{4}$$

with

$$\left\{ \begin{array}{rcl} \mathbf{A_1^0 A_2^0} & = & \mathbf{q_{02} x_B} \\ \mathbf{A_1^0 A_3^0} & = & \mathbf{q_{03} x_B} + 2H\mathbf{y_B} \\ \mathbf{A_1^0 A_4^0} & = & \mathbf{q_{04} x_B} + 2H\mathbf{y_B} \end{array} \right.$$

Consequently the kinematic parameters in the base frame R_B are determined by nonlinear minimization of the error function F_1:

$$F_1(\mathbf{q_{02}}, \mathbf{q_{03}}, \mathbf{q_{04}}, H) = \sum_{(\mathbf{p},\mathbf{q}),\mathbf{p}>\mathbf{q}} [\mathbf{V_p}.\mathbf{V_q}|_{R_C} - \mathbf{V_p}.\mathbf{V_q}|_{R_B}]^2 \tag{5}$$

with $\mathbf{V_p}$ and $\mathbf{V_q}$ two elements of $\mathbf{V}$ and $\cdot|_R$ representing the frame R used to express the terms of $\mathbf{V}$.

Six independent equations can be expressed from the elements of $\mathbf{V}$, which ensures the identifiability of the four kinematic parameters.

At the end of this second step, the four parameters $(\mathbf{q_{02}}, \mathbf{q_{03}}, \mathbf{q_{04}}, H)$ related to the actuators and the location of the points $\mathbf{A_j},\ \mathbf{j} \in [1,4]$ are identified.

3.3 Step 3 - Identification of the length of the elements connected to the end-effector

From the first step, one can express the position of the joint center $\mathbf{A_j}$ for any end-effector pose. The position of the joint center $\mathbf{B_j}$ can hence be written in the camera frame as a function of the length L of the kinematically equivalent single rods connected to the traveling plate:

$$\mathbf{B_{j,k}}|_{R_C} = \mathbf{A_{j,k}}|_{R_C} + L\underline{\mathbf{u}}_{\mathbf{j,k}}|_{R_C},\ \mathbf{k} \in [1,N] \tag{6}$$

with N the number of used end-effector poses, $\mathbf{B_{j,k}}$ the position of $\mathbf{B_j},\ \mathbf{j} \in [1,4]$ for the k-th end-effector pose and $\underline{\mathbf{u}}_{\mathbf{j,k}}$ the unit vector of the axis of the observed element, determined from its image. An error function is introduced by considering like Notash [16] the invariance of the distances between the points $\mathbf{B_j}$ between two consecutive end-effector poses k and k+1. The invariance of the distances $\|\mathbf{B_1 B_2}\|$ and $\|\mathbf{B_3 B_4}\|$ can be expressed by:

$$\left.\begin{array}{l} \|\mathbf{B_{1,k+1} B_{2,k+1}}\|_{R_C} = \|\mathbf{B_{1,k} B_{2,k}}\|_{R_C} \\ \|\mathbf{B_{3,k+1} B_{4,k+1}}\|_{R_C} = \|\mathbf{B_{3,k} B_{4,k}}\|_{R_C} \end{array}\right\}\ \mathbf{k} \in [1, N_I - 1] \tag{7}$$

The length L of the elements connected to the end-effector is therefore determined by nonlinear minimization of the error function F_2:

$$F_2(L) = \sum_{\mathbf{k}=1}^{N_I-1} \Big[\left(\|\mathbf{B_{1,k+1} B_{2,k+1}}\|^2_{R_C} - \|\mathbf{B_{1,k} B_{2,k}}\|^2_{R_C}\right)^2 + \left(\|\mathbf{B_{3,k+1} B_{4,k+1}}\|^2_{R_C} - \|\mathbf{B_{3,k} B_{4,k}}\|^2_{R_C}\right)^2\Big]$$

At the end of the third step, the length of the kinematically equivalent single rods connected to the traveling plate is identified. It is important to notice that this step is independent from the previous one. No error propagation hence occurs.

3.4 Step 4 - Parameter estimation in the end-effector frame

In the fourth step, the parameters related to the traveling plate are identified. The previous step enables one to determine the values of the distances $\|\mathbf{B_1 B_2}\|$ and $\|\mathbf{B_3 B_4}\|$. These distances only depend on the parameter S, which is therefore immediately determined.

To determine the other dimension D, the relative displacement of the two traveling plate elements has to be taken into account. The distance between $\mathbf{B_1}$ (resp. $\mathbf{B_3}$) and $\mathbf{B_2}$ (resp. $\mathbf{B_4}$) along $\mathbf{y_B}$ is constant and known in the camera frame, with for instance:

$$\mathbf{B_1 B_3}.\mathbf{y_B} = -L\underline{\mathbf{u}}_{\mathbf{1,k}}.\mathbf{y_B} + 2(H - D) + L\underline{\mathbf{u}}_{\mathbf{3,k}}.\mathbf{y_B},\ \forall \mathbf{k} \tag{8}$$

The corresponding distance $2D$ is hence also immediately identified since all the other terms in (8) are known at this point.

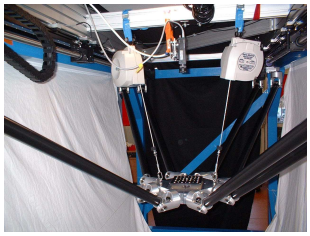

Figure 4: *Experimental setup*

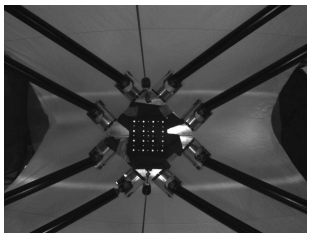

Figure 5: *Leg image with the camera.*

Parameter	L (m)	H (m)	D (m)	S (m)
A priori	1.0010	0.5000	0.1536	0.1536
Identified	1.0213	0.4985	0.1602	0.1598
Parameter	$\mathbf{q_{0_2}}$ (m)	$\mathbf{q_{0_3}}$ (m)	$\mathbf{q_{0_4}}$ (m)	
A priori	1.5705	1.2190	2.8700	
Identified	1.5675	1.2190	2.7867	

Table 2: *A priori and identified kinematic parameters*

Parameter set	Mean	Root mean square
a priori	-0.06mm	0.53mm
Identified	-3.4E-3mm	0.33 mm

Table 3: *Gaps between vision-based end-effector displacement measurements and their estimation computed from a kinematic parameter set.*

4 Experimental results

4.1 Experimental setup

The camera is located on the base of the mechanism so that the four legs are observable, as well as a calibration board linked to the end-effector (figures 4 and 5). The camera has a resolution of 1024×768pixels, 8-bit encoded, with a 3.6mm lens. The calibration board enables one to perform end-effector pose measurements to evaluate the calibration efficiency.

Five poses are considered for each joint location determination in step 1. Another 20-pose set is used for the steps 2 to 4.

4.2 Experimental results

The determination of the spherical joint positions in the camera frame (step 1) is achieved with an accuracy in the order of $1mm$. The identified kinematic parameters are indicated in table 2 with the *a priori* values. The parameter value modifications are noticeable, with variations in the order of several millimeters.

4.3 Validation tests

End-effector displacement analysis. Observation of the calibration board enables us to measure its pose with respect to the camera. The end-effector displacement between two poses can therefore be estimated from these pose measurements. On the other hand, the end-effector displacement can be estimated using the direct kinematic model, the proprioceptive sensor values recorded during the experiment and a kinematic parameter set, either identified or estimated *a priori*. In table 3, the mean and root mean squares of the gaps between the vision-based displacement measurements and their estimation are indicated for the parameters identified with the proposed method. The gaps are computed for the 20-pose set used for calibration. The identified parameters enable us to lower significantly the gaps between the measured end-effector displacements and their estimation.

Kinematic constraint. An independent validation test has been also achieved by imposing a kinematic constraint on the end-effector (Figure 6). The end-effector is manually constrained to follow a line materialized by a ruler. The corresponding joint variables are stored. From these joint variable values, poses are computed by means of the direct kinematic model. The physical setup implies that these poses should lie on a straight line. Hence, the straightness of the line is computed for the kinematic parameter sets (*a priori* and identified) as the root mean square of the distance between the different positions and the line estimated by a least squares criterion.

A $500mm$ line is measured. The straightness measurement repeatability, experimentally evaluated equal to 0.07mm, is in the order of the improvement induced by the calibration (table 4). The accuracy improvement can hence not be concluded using this second evaluation criterion. This experiment demonstrates the difficulties that might be encountered while using

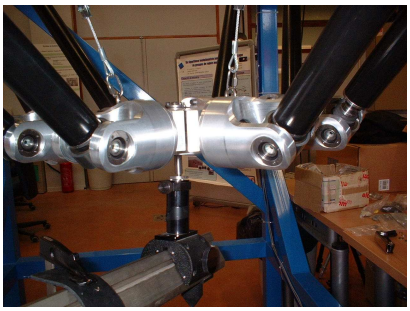

Figure 6: *Experimental set-up for the straightness evaluation.*

Parameter set	Straightness
a priori	0.53mm
Identified	0.50mm

Table 4: *Straightness evaluation with the a priori and identified kinematic parameter sets.*

a kinematic constraint to achieve the calibration of a mechanism with large workspace.

5 Conclusion

Parallel mechanisms with linear actuators on the base are of great interest for applications where high dynamics are required. Like serial mechanisms, they need a kinematic calibration to improve their accuracy. In this article, we proposed an original approach to achieve the calibration process, observing the legs with a camera. The ease of use and the absence of mechanism modifications due to the use of an exteroceptive sensor are combined to the advantage of having information directly bound to the mechanism kinematics, like methods based on the use of redundant proprioceptive sensors. The method has been developed in the context of the calibration of a I4 parallel mechanism, with a noticeable accuracy improvement according to vision-based pose measurement. Future work will now concern the accuracy improvement when considering the dynamics of the end-effector.

Acknowledgment

This study was jointly funded by CPER Auvergne 2001-2003 program and by the MAX project within the CNRS-ROBEA program.

References

[1] M. Honegger, A. Codourey, and E. Burdet, "Adaptive control of the hexaglide, a 6 dof parallel manipulator," in *Proc. of the 1997 IEEE Int. Conf. on Robotics and Automation*, Albuquerque, New Mexico, april 1997, pp. 543–548.

[2] S. Krut, O. Company, M. Benoit, H. Ota, and F. Pierrot, "I4: A new parallel mechanism for Scara motions," in *Proc. of the 2003 Int. Conf. on Robotics and Automation*, Taipei, Taiwan, september 2003, pp. 1875–1880.

[3] D. Chablat and P. Wenger, "Architecture optimization of a 3-DOF parallel mechanism for machining applications, the Orthoglide," *IEEE Trans. on Robotics and Automation*, vol. 19, no. 3, pp. 403–410, june 2003.

[4] J.-P. Merlet, *Parallel Robots*. Kluwer Academic Publishers, 2000, ISBN 0-7923-6308-6.

[5] J. Wang and O. Masory, "On the accuracy of a Stewart platform - Part I: The effect of manufacturing tolerances," in *Proc. of the 1993 IEEE Int. Conf. on Robotics and Automation*, Atlanta, Georgia, 1993, pp. 114–120.

[6] D. Daney, "Etalonnage géométrique des robots parallèles," Ph.D. dissertation, Université de Nice - Sophia Antipolis, 2000.

[7] P. Renaud, N. Andreff, F. Marquet, and P. Martinet, "Vision-based kinematic calibration of a H4 parallel mechanism," in *Proc. of the 2003 IEEE Int. Conf. on Robotics and Automation*, Taipei, Taiwan, september 2003, pp. 1191–1196.

[8] C. Wampler and T. Arai, "Calibration of robots having kinematic closed loops using non-linear least-squares estimation," in *Proc. of the 1992 IFTOMM World Congress in Mechanism and Machine Science*, Nagoya, Japan, September 1992, pp. 153–158.

[9] H. Zhuang, "Self-calibration of parallel mechanisms with a case study on Stewart platforms," *IEEE Trans. on Robotics and Automation*, vol. 13, no. 3, pp. 387–397, 1997.

[10] H. Zhuang and L. Liu, "Self calibration of a class of parallel manipulators," in *Proc. of the 1996 IEEE Int. Conf. on Robotics and Automation*, Minneapolis, Minnesota, 1996, pp. 994–999.

[11] W. Khalil and D. Murareci, "Autonomous calibration of parallel robots," in *Proc. of the* 5^{th} *IFAC Symp. on Robot Control*, Nantes, France, 1997, pp. 425–428.

[12] W. Khalil and S. Besnard, "Self calibration of Stewart-Gough parallel robots without extra sensors," *IEEE Trans. on Robotics and Automation*, vol. 15, no. 6, pp. 1116–1121, 1999.

[13] D. Daney, "Self calibration of Gough platform using leg mobility constraints," in *Proc. of the* 10^{th} *World Congress on the theory of machine and mechanisms*, Oulu, Finland, 1999, pp. 104–109.

[14] P. Renaud, N. Andreff, G. Gogu, and P. Martinet, "On vision-based kinematic calibration of n-leg parallel mechanisms," in *Proceedings of IFAC Symposium on System Identification 2003*, Rotterdam, Pays-Bas, august 2003.

[15] P. Renaud, "Apport de la vision pour l'identification géométrique de mécanismes parallèles," Ph.D. dissertation, Université Blaise Pascal, Clermont-Ferrand, France, 2003.

[16] L. Notash and R. Podhorodeski, "Fixtureless calibration of parallel manipulators," *Trans. of the CSME*, vol. 21, no. 3, pp. 273–294, 1997.